



First results from the Imaging Motional Stark Effect diagnostic on ASDEX Upgrade

40th European Physical Society Conference on Plasma Physics
Espoo, Finland, July 2013

O. P. Ford,¹ J. Howard,² M. Reich,¹ J. Hobirk,¹
J. Svensson,¹ R. Wolf,¹ ASDEX Upgrade Team

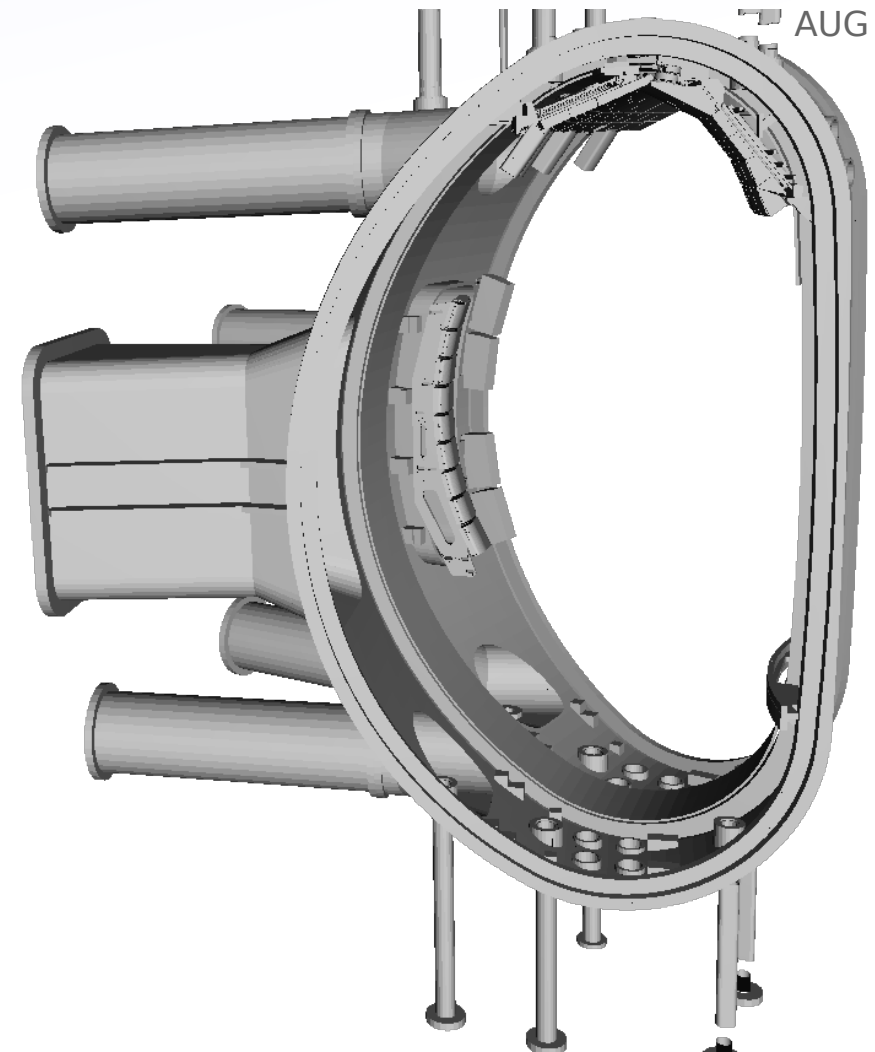
1: Max-Planck Institut für Plasmaphysik, Greifswald/Garching, Germany

2: Plasma Research Laboratory, Australian National University, Canberra



(Imaging) Motional Stark Effect at AUG

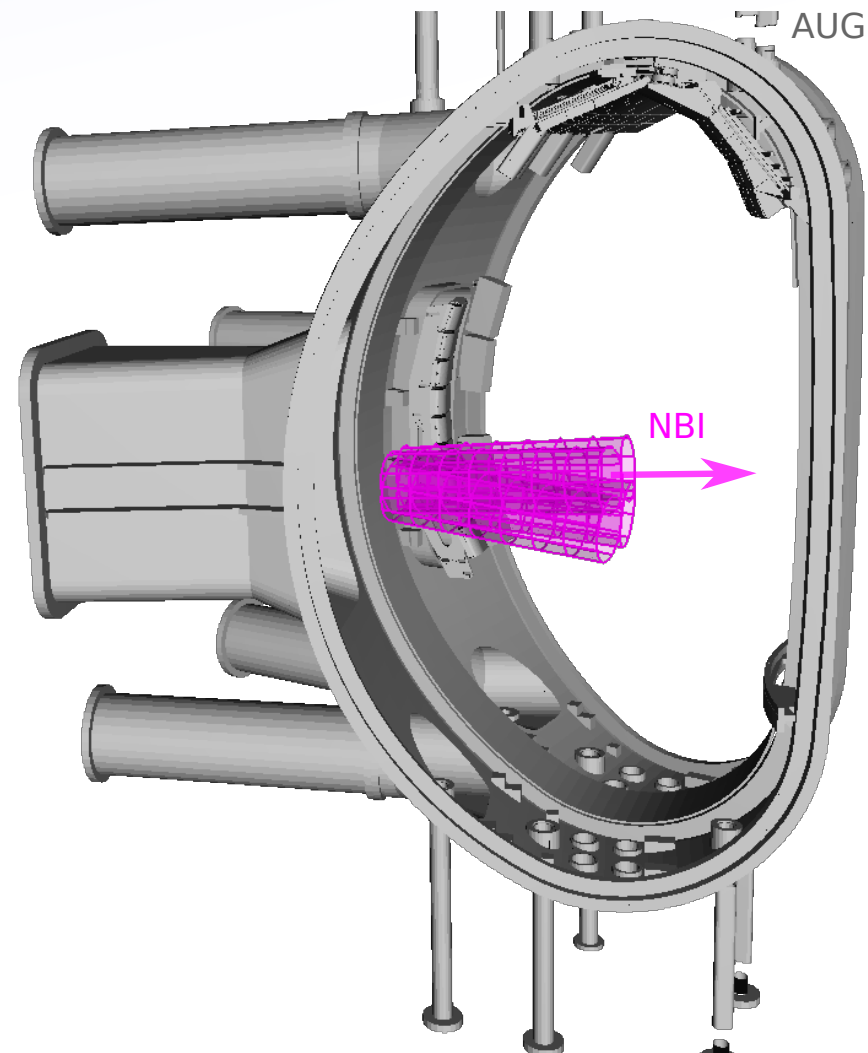
ASDEX Upgrade has an existing 10-channel MSE system.



(Imaging) Motional Stark Effect at AUG

ASDEX Upgrade has an existing 10-channel MSE system.

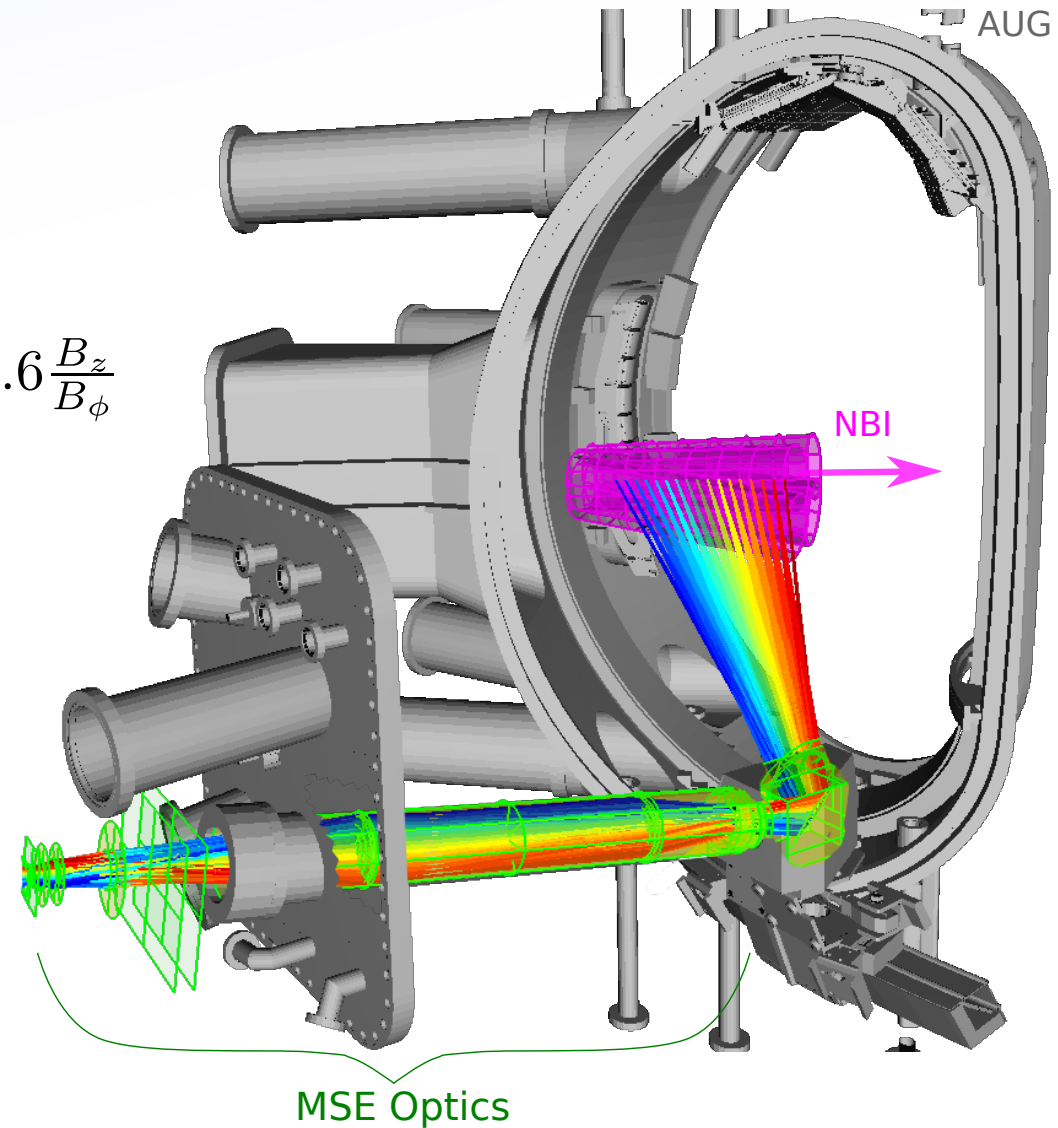
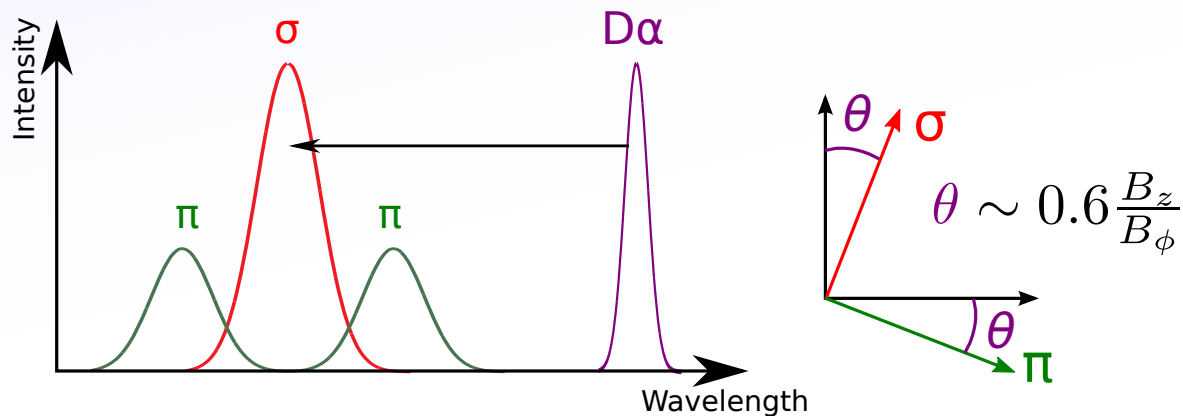
$H\alpha/D\alpha$ beam emission is Doppler shifted by beam velocity and split by the Motional Stark Effect into π and σ components which are polarised perpendicular and parallel to projected $\mathbf{v} \times \mathbf{B}$ direction:



(Imaging) Motional Stark Effect at AUG

ASDEX Upgrade has an existing 10-channel MSE system.

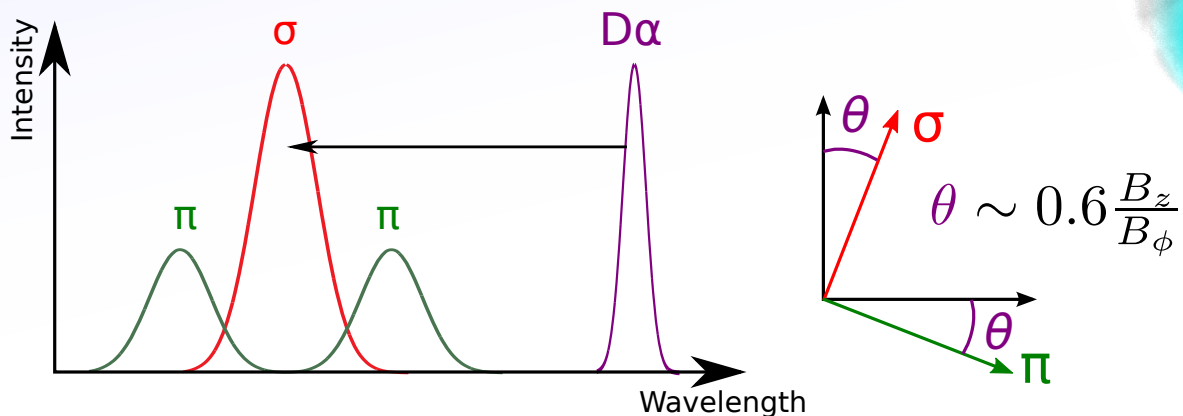
H α /D α beam emission is Doppler shifted by beam velocity and split by the Motional Stark Effect into π and σ components which are polarised perpendicular and parallel to projected $\mathbf{v} \times \mathbf{B}$ direction:



(Imaging) Motional Stark Effect at AUG

ASDEX Upgrade has an existing 10-channel MSE system.

H α /D α beam emission is Doppler shifted by beam velocity and split by the Motional Stark Effect into π and σ components which are polarised perpendicular and parallel to projected $\mathbf{v} \times \mathbf{B}$ direction:



The IMSE observes a full image of the beam emission using a CCD camera, giving $> 60 \times 60$ θ measurements.

As well as the increase in data, the 2D spread can be shown to give more information for current inference (tomographic reconstruction)

It replaced the MSE for two short periods of plasma operation this year with the objective of testing the basic principle.

Modelled Image

Conventional MSE

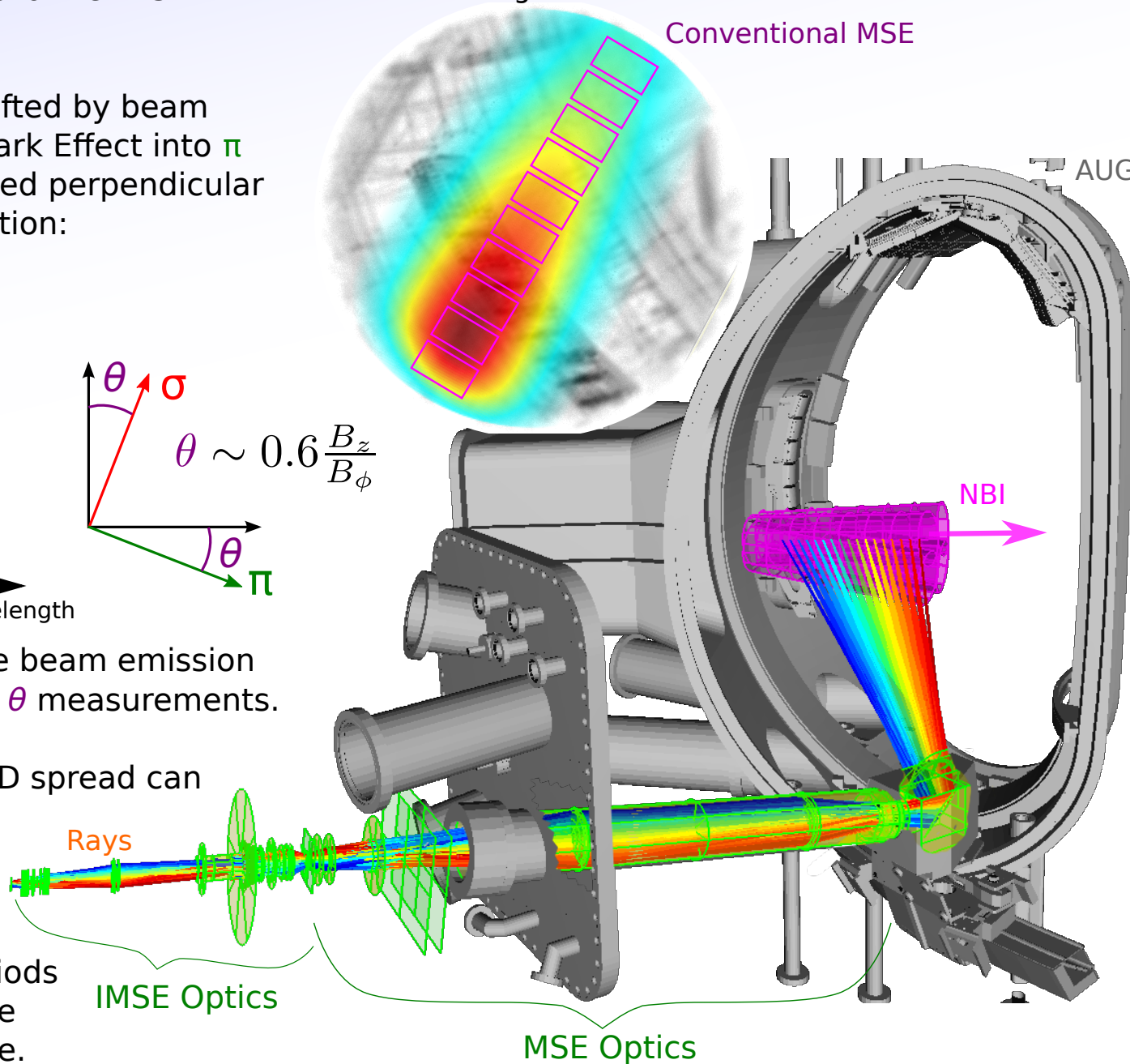
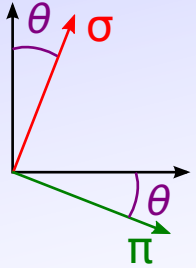


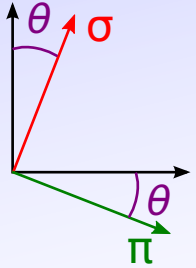
Image Demodulation



Two birefringent plates modulate the image with orthogonal interference patterns. The difference in the wavelength of the σ and π components is exploited to cause their interference patterns to add. Since the measurement of θ is periodic in 90° , the angle θ from each of the σ and π are averaged.

(Details in P6.006 poster, Diagnostics Satellite Meeting, Saturday)

Image Demodulation



Two birefringent plates modulate the image with orthogonal interference patterns. The difference in the wavelength of the σ and π components is exploited to cause their interference patterns to add. Since the measurement of θ is periodic in 90° , the angle θ from each of the σ and π are averaged.

(Details in P6.006 poster, Diagnostics Satellite Meeting, Saturday)

The image produced follows:

$$I \propto 1 + \zeta \cos(2\theta) \cos(x) + \zeta \sin(2\theta) \cos(x+y) + \zeta \sin(2\theta) \cos(x-y)$$

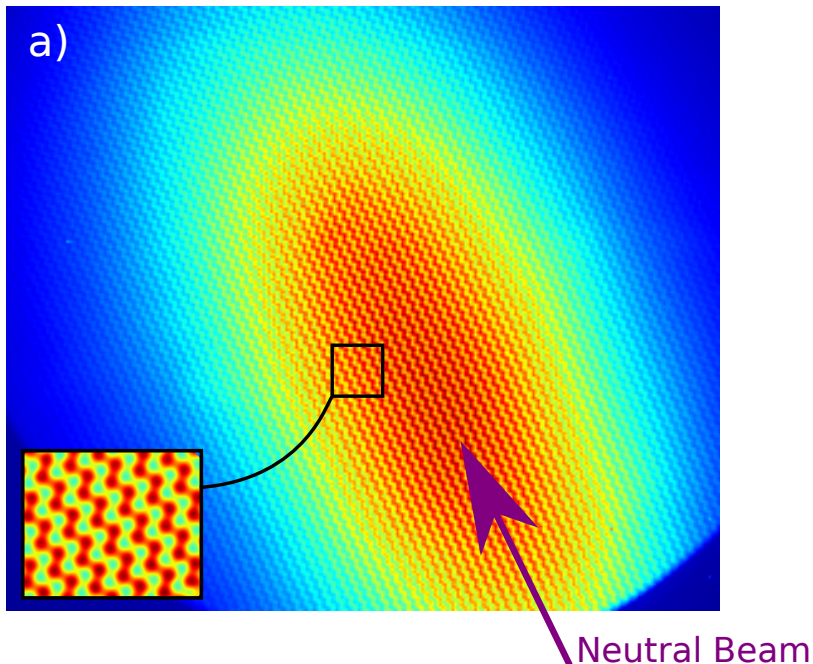
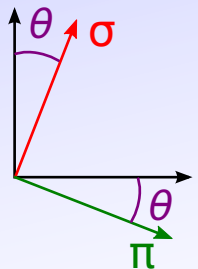


Image Demodulation



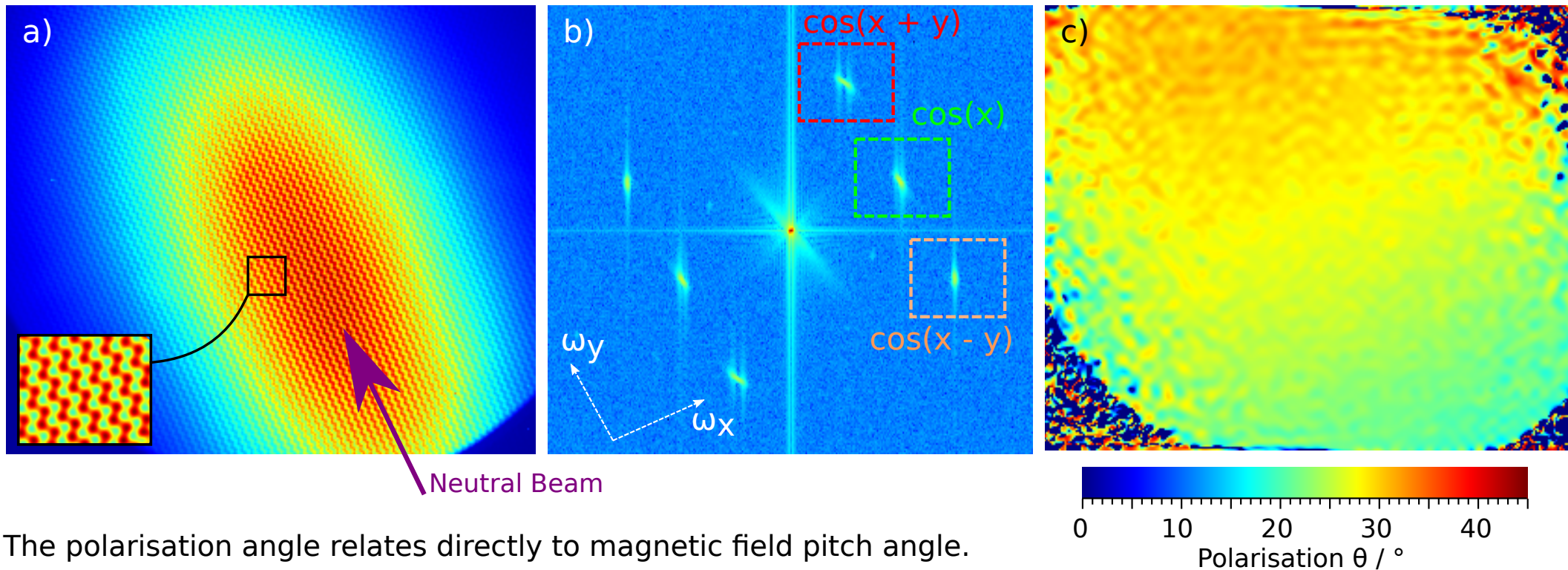
Two birefringent plates modulate the image with orthogonal interference patterns. The difference in the wavelength of the σ and π components is exploited to cause their interference patterns to add. Since the measurement of θ is periodic in 90° , the angle θ from each of the σ and π are averaged.

(Details in P6.006 poster, Diagnostics Satellite Meeting, Saturday)

The image produced follows:

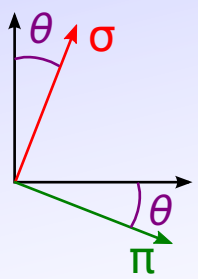
$$I \propto 1 + \zeta \cos(2\theta) \cos(x) + \zeta \sin(2\theta) \cos(x+y) + \zeta \sin(2\theta) \cos(x-y)$$

The three components can be easily isolated from the 2D Fourier Transform:



The polarisation angle relates directly to magnetic field pitch angle.

Image Demodulation



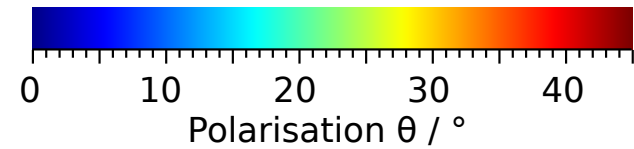
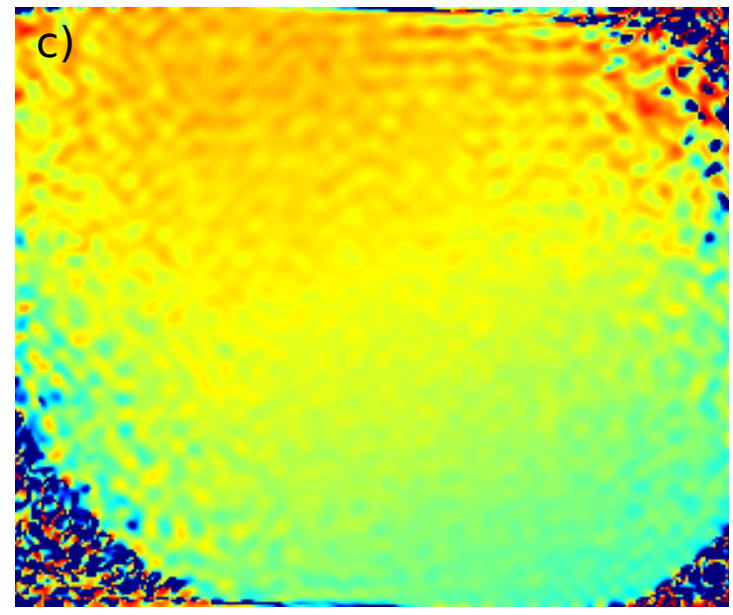
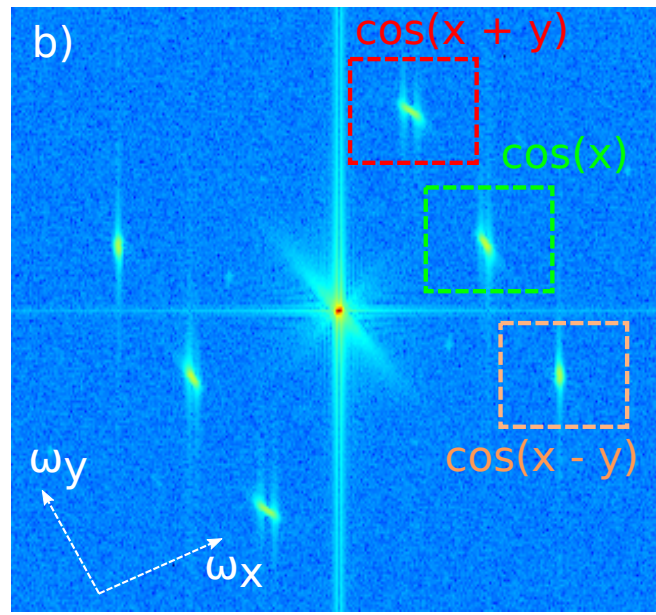
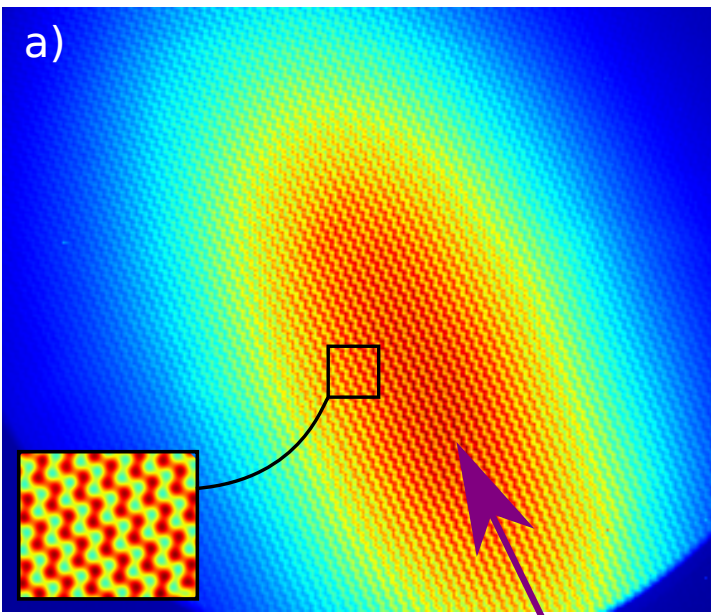
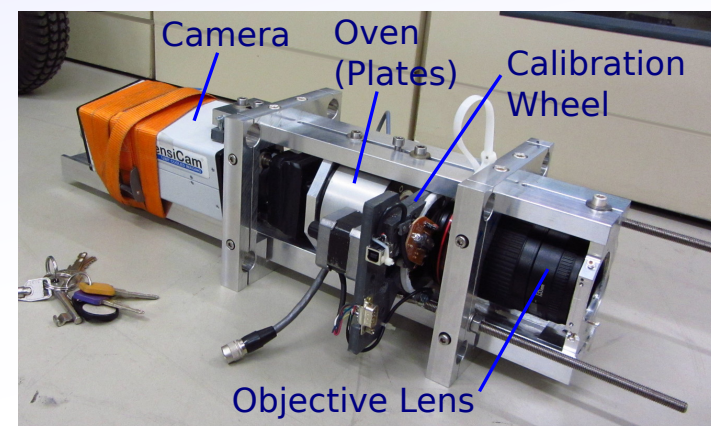
Two birefringent plates modulate the image with orthogonal interference patterns. The difference in the wavelength of the σ and π components is exploited to cause their interference patterns to add. Since the measurement of θ is periodic in 90° , the angle θ from each of the σ and π are averaged.

(Details in P6.006 poster, Diagnostics Satellite Meeting, Saturday)

The image produced follows:

$$I \propto 1 + \zeta \cos(2\theta) \cos(x) + \zeta \sin(2\theta) \cos(x+y) + \zeta \sin(2\theta) \cos(x-y)$$

The three components can be easily isolated from the 2D Fourier Transform:



The polarisation angle relates directly to magnetic field pitch angle.

Image Transform

The imaging nature of the system allows easy position calibration by identifying known features in a background image and calculating the intersection with the neutral beam:

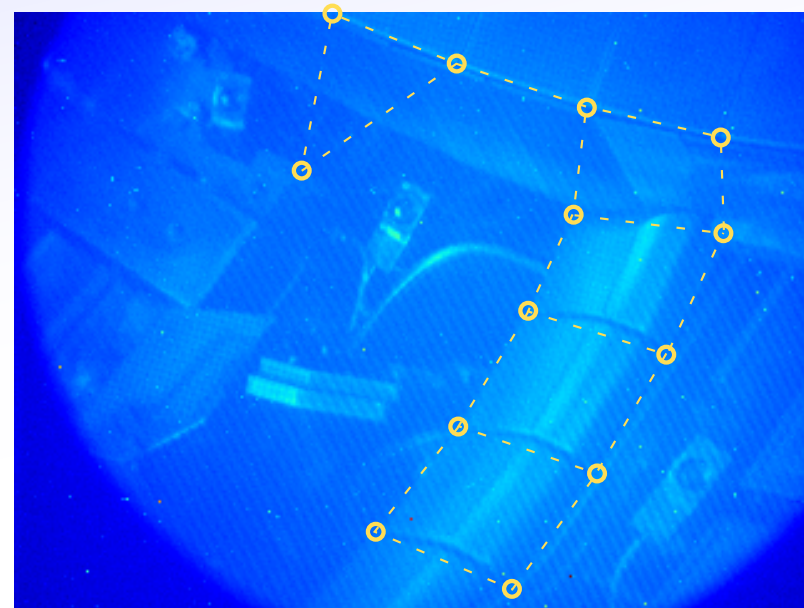
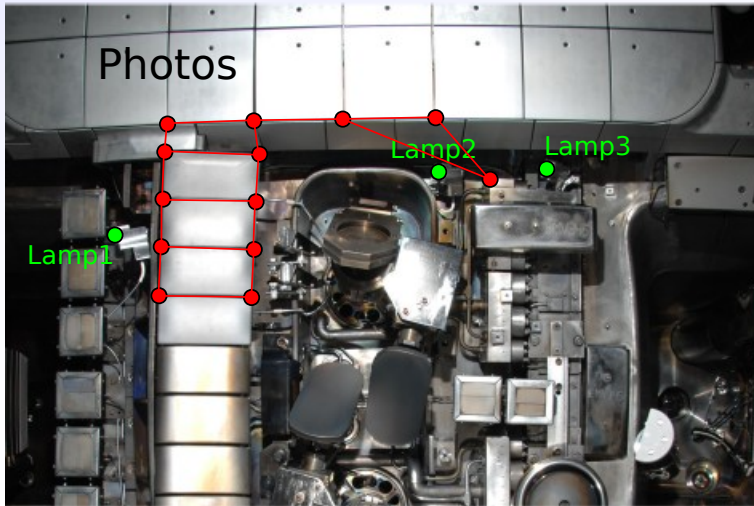
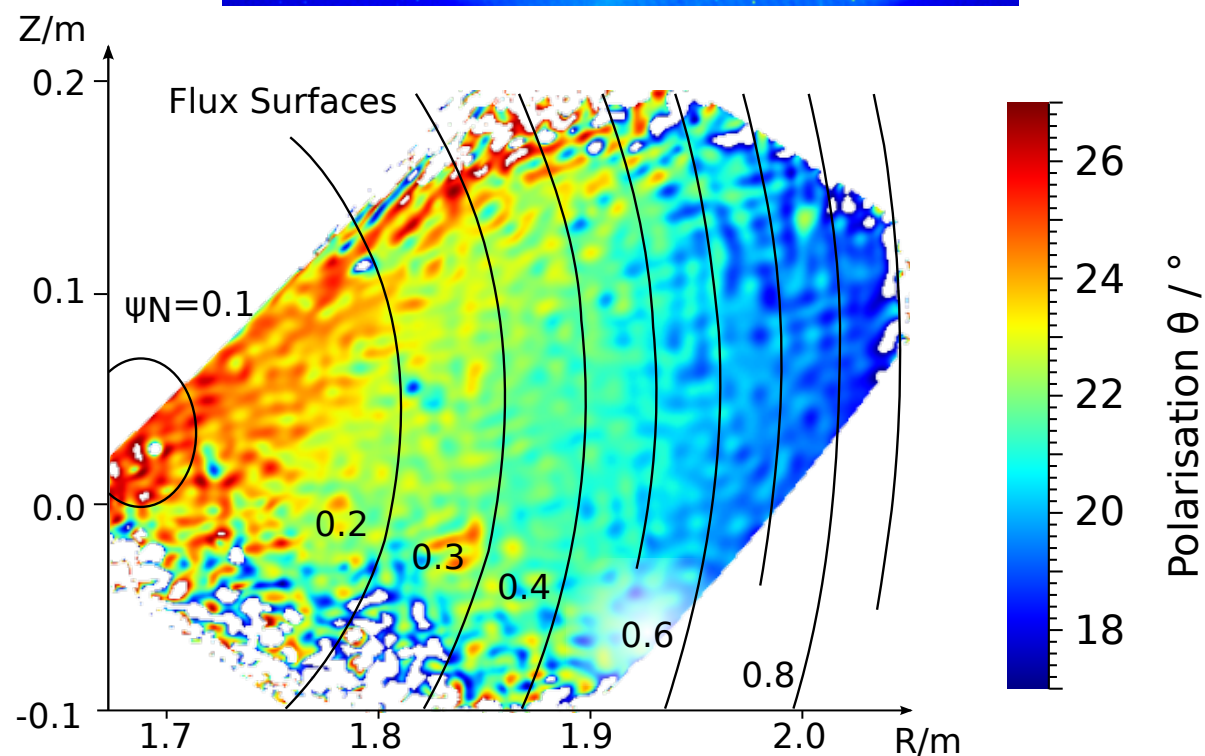
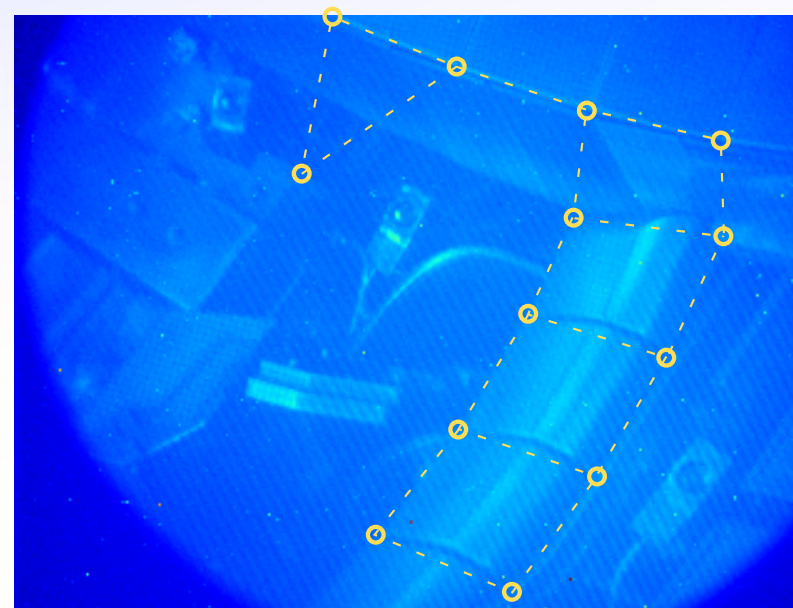
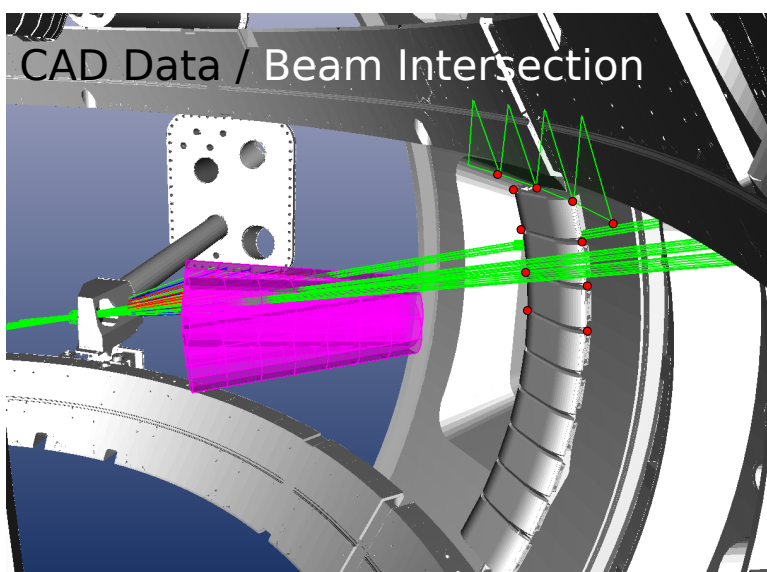
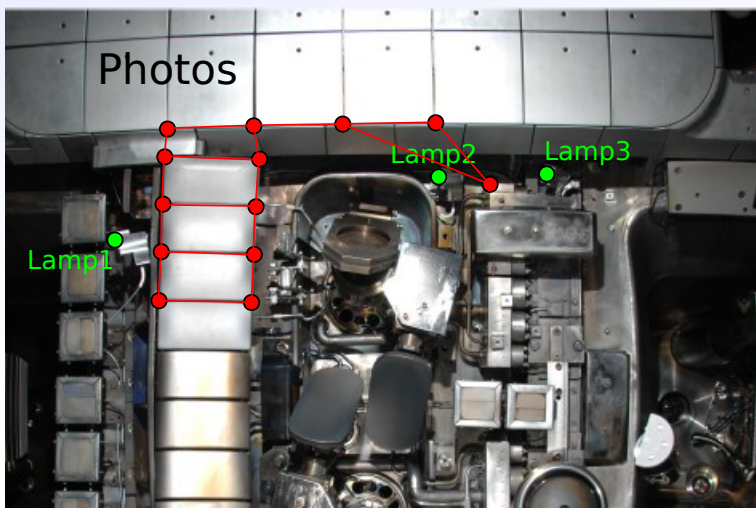


Image Transform

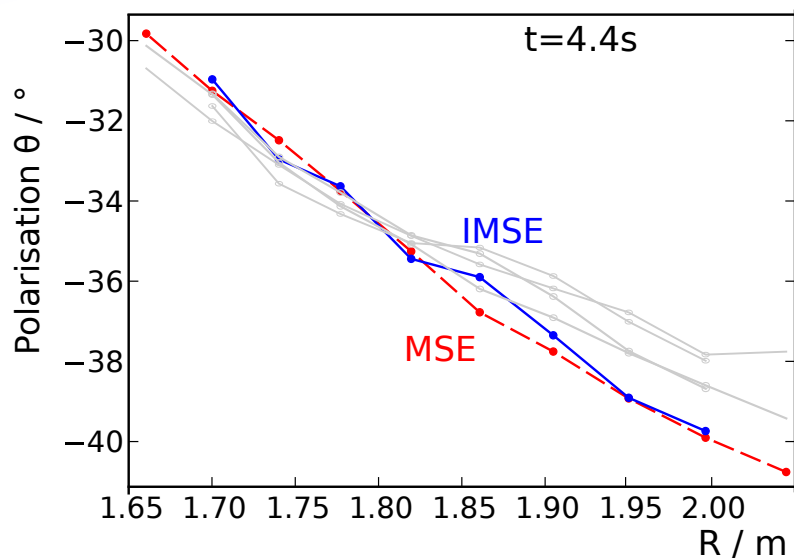
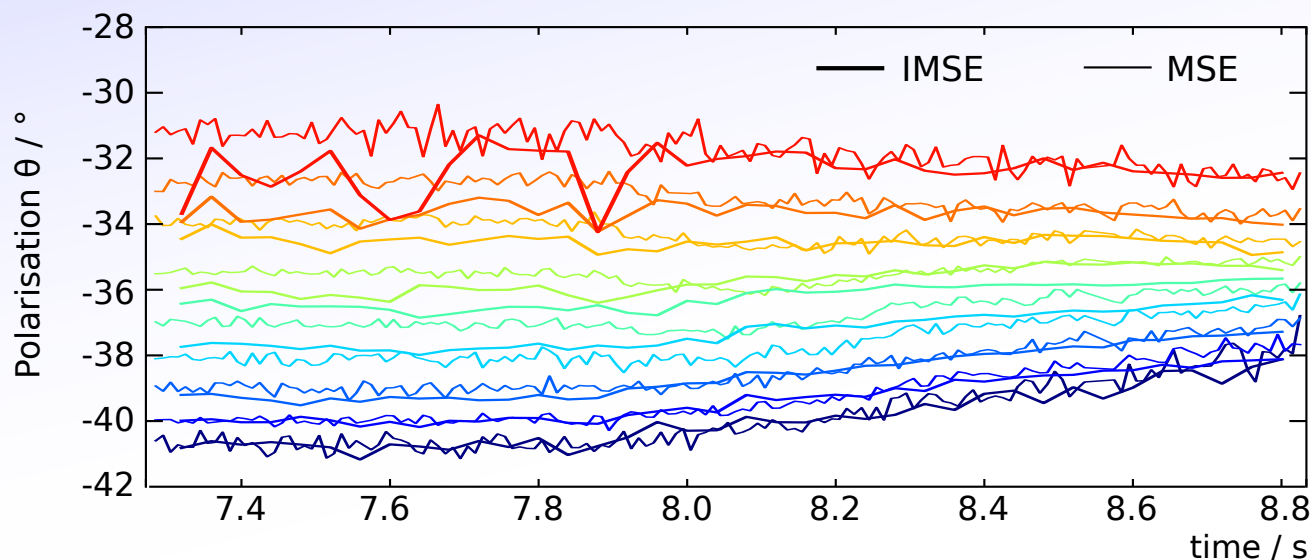
The imaging nature of the system allows easy position calibration by identifying known features in a background image and calculating the intersection with the neutral beam:





Direct MSE - IMSE comparison

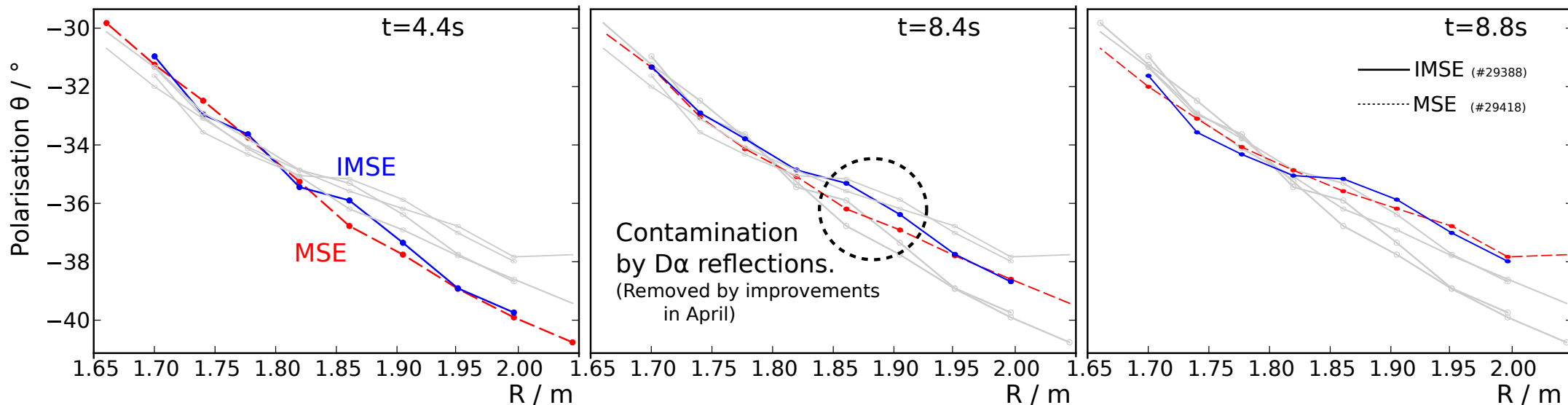
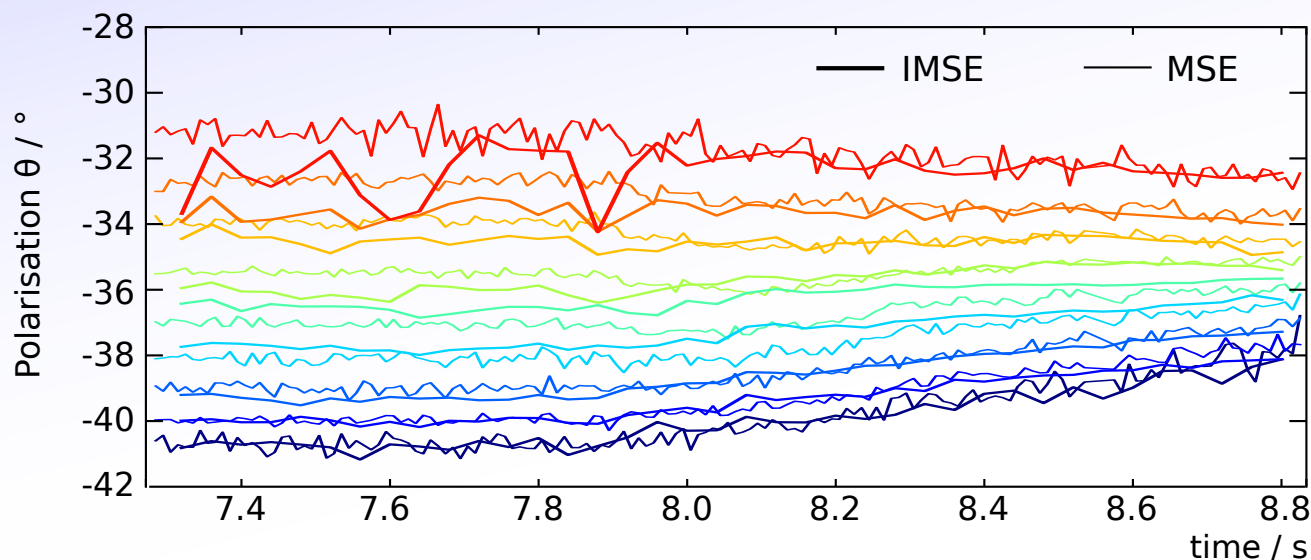
To compare the IMSE and MSE systems directly, the same plasma shot was run with the MSE system in the following week. Except for a 1.1° offset, the agreement is good:

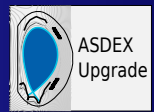




Direct MSE - IMSE comparison

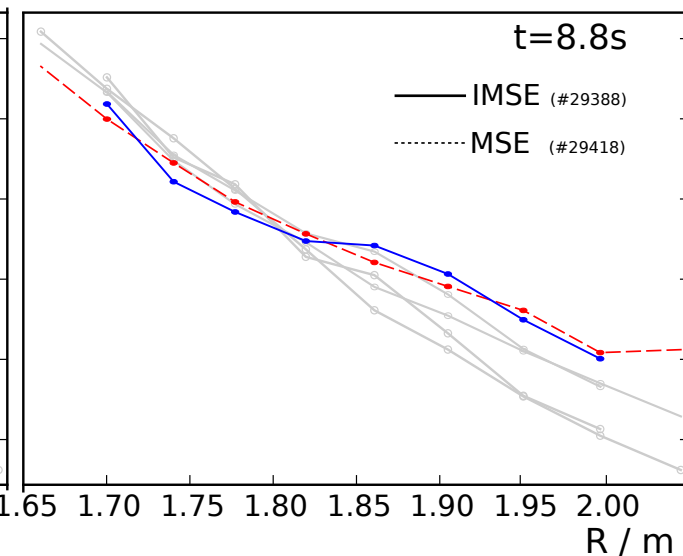
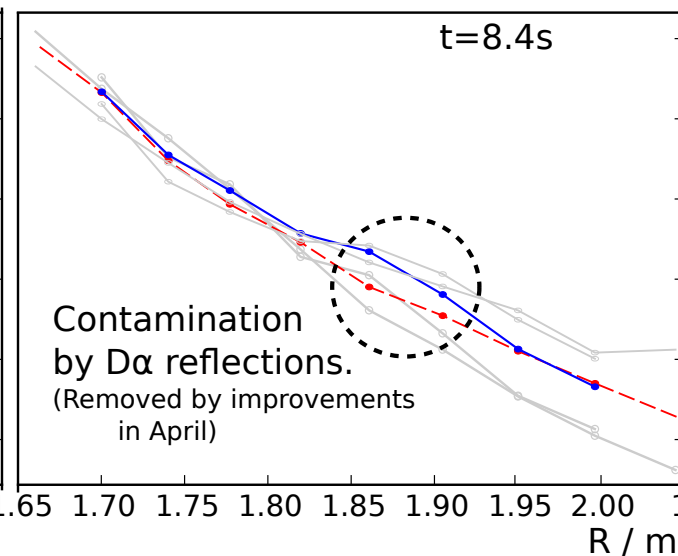
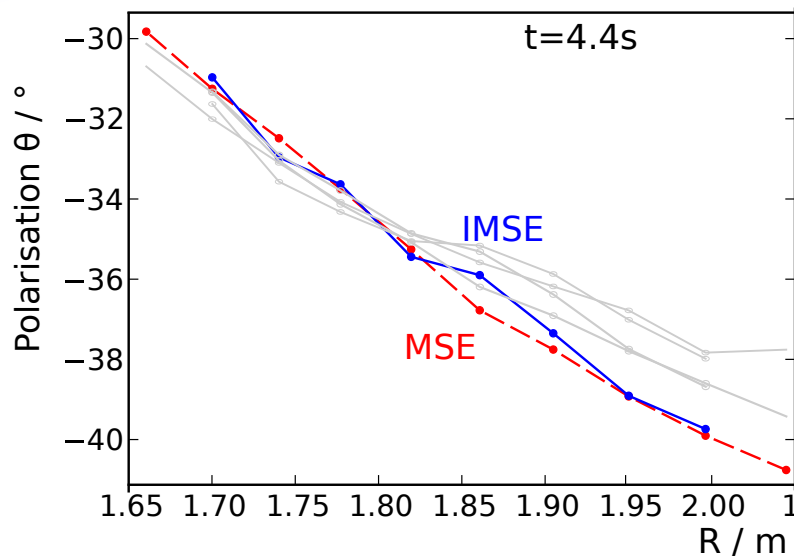
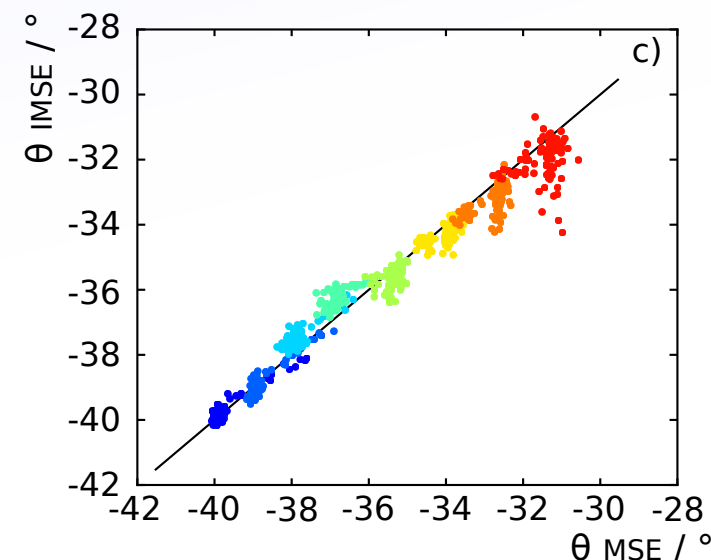
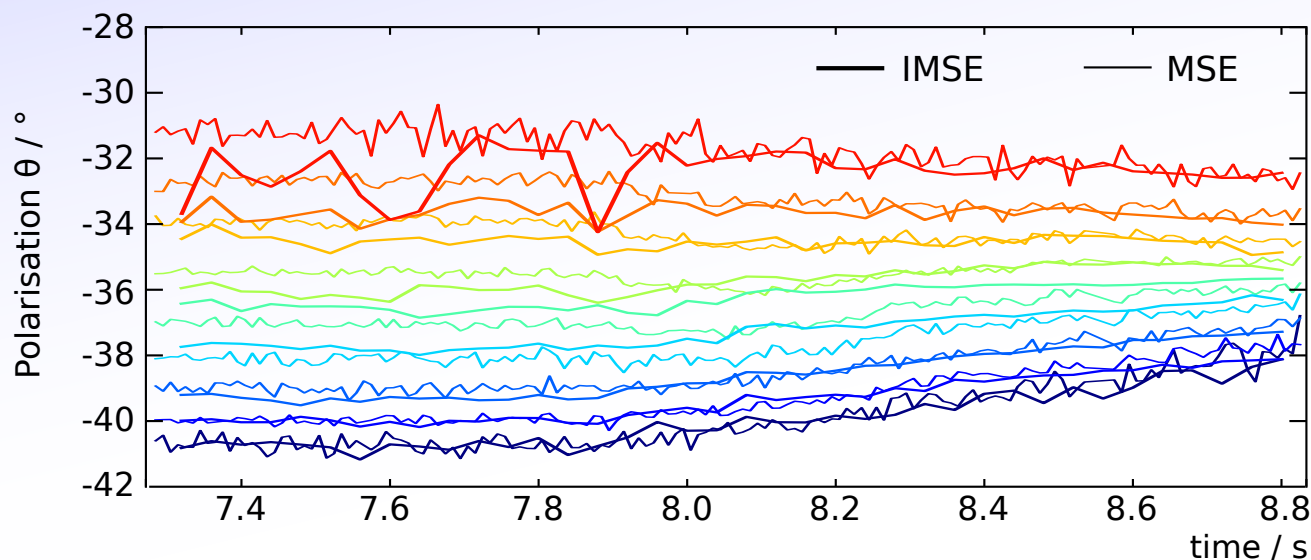
To compare the IMSE and MSE systems directly, the same plasma shot was run with the MSE system in the following week. Except for a 1.1° offset, the agreement is good:





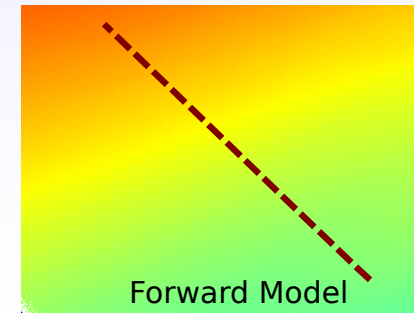
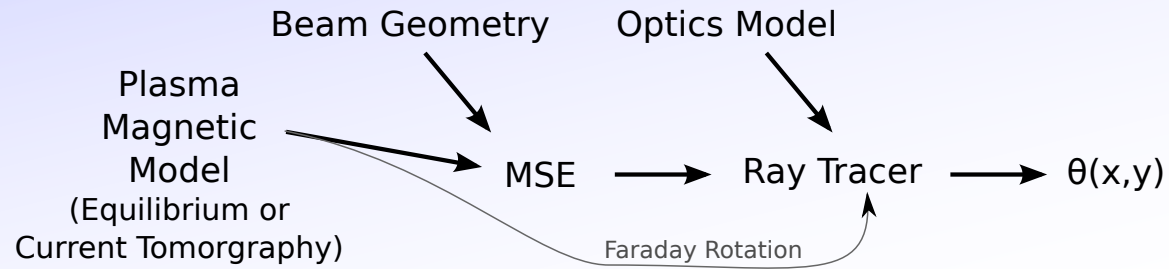
Direct MSE - IMSE comparison

To compare the IMSE and MSE systems directly, the same plasma shot was run with the MSE system in the following week. Except for a 1.1° offset, the agreement is good:



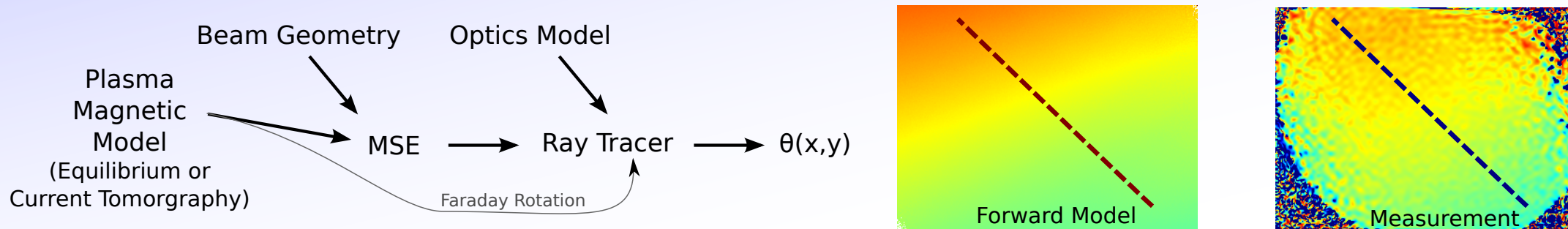
Comparison with Forward Model

For the design and analysis, a full forward model of the system was built (up to polarisation angle at IMSE):

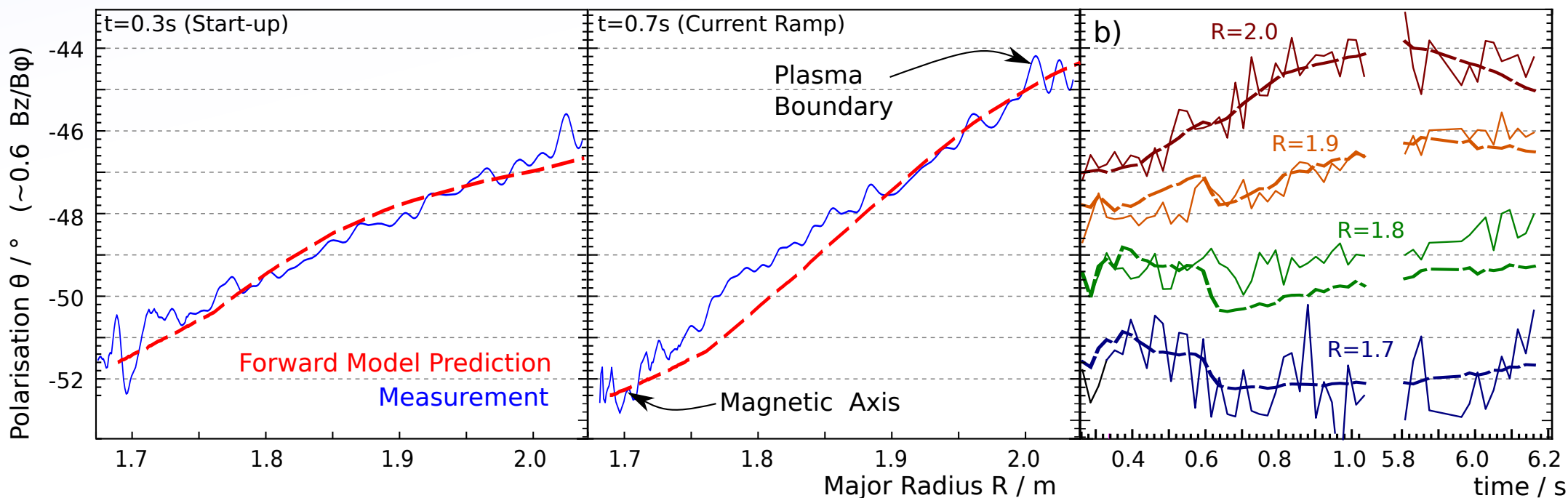


Comparison with Forward Model

For the design and analysis, a full forward model of the system was built (up to polarisation angle at IMSE):



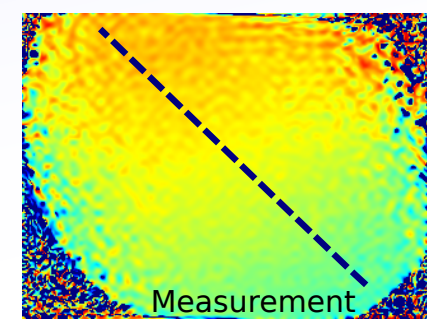
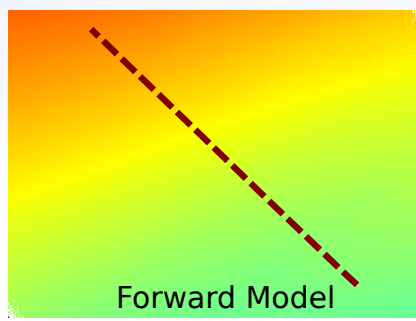
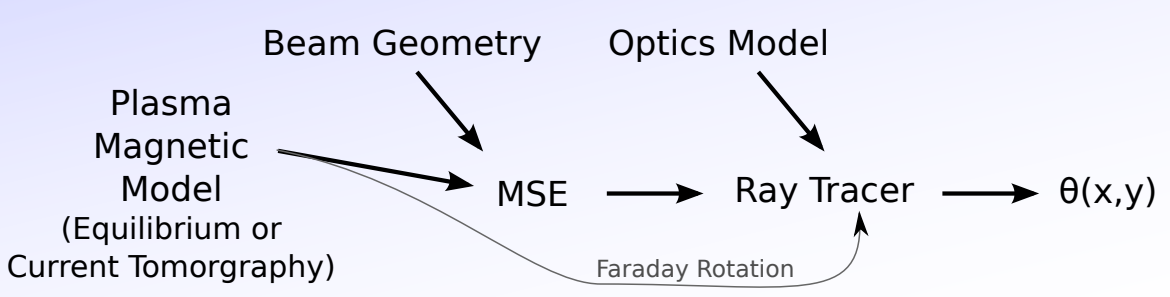
Compared directly with the measurement, there is only a 0.7° offset. Once subtracted, it agrees during current ramp with the regions where the equilibrium/CT is expected to correctly predict the pitch angle:



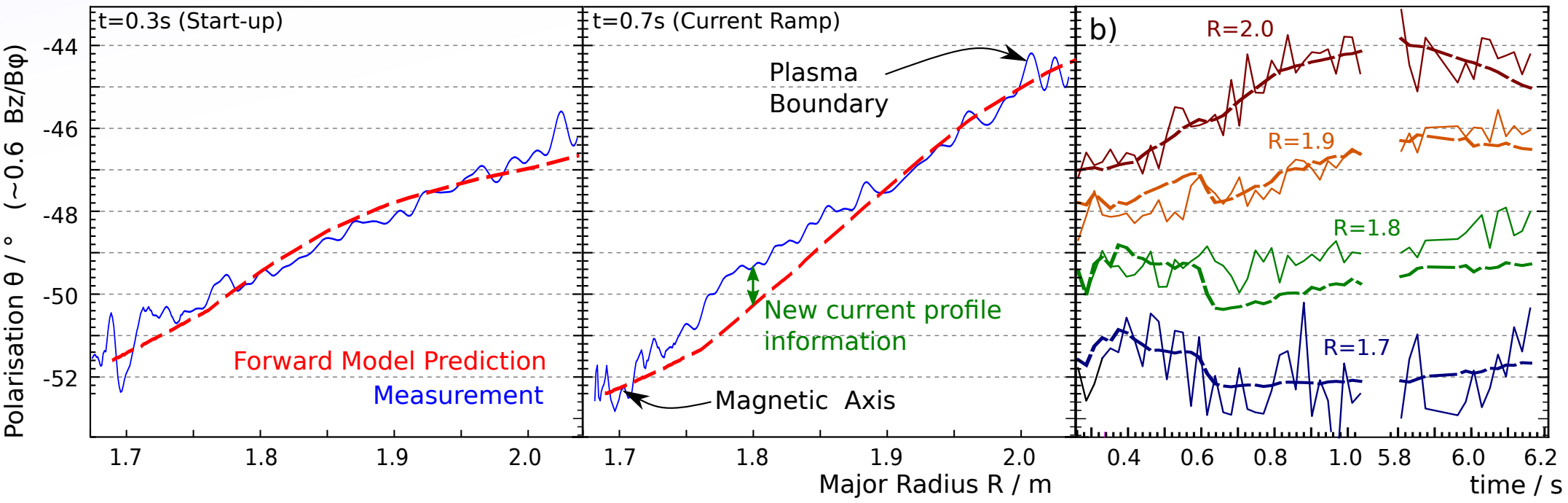
At present, the diagnostic has **no angle calibration**. The forward model is based entirely on the CAD and optics models and the measurement is unprocessed.

Comparison with Forward Model

For the design and analysis, a full forward model of the system was built (up to polarisation angle at IMSE):



Compared directly with the measurement, there is only a 0.7° offset. Once subtracted, it agrees during current ramp with the regions where the equilibrium/CT is expected to correctly predict the pitch angle:

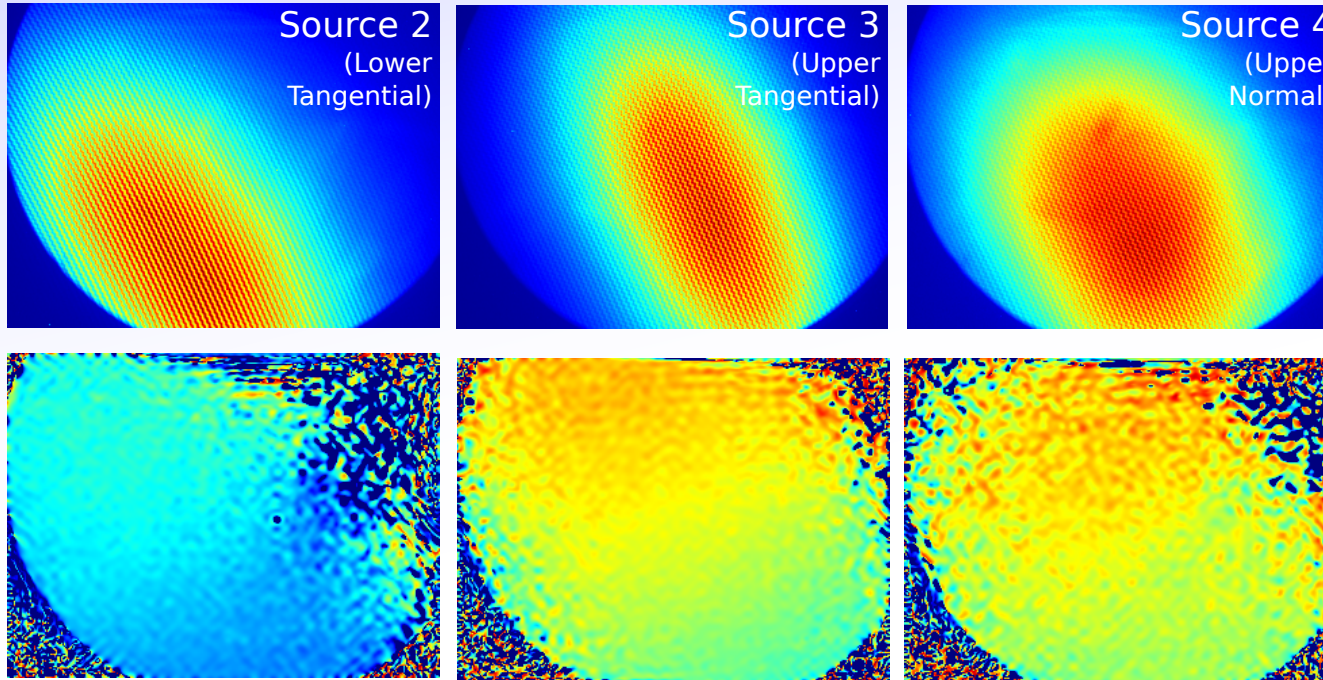


At present, the diagnostic has **no angle calibration**. The forward model is based entirely on the CAD and optics models and the measurement is unprocessed. The disagreement at mid-radius is useful information that will be used to constrain the current profile.



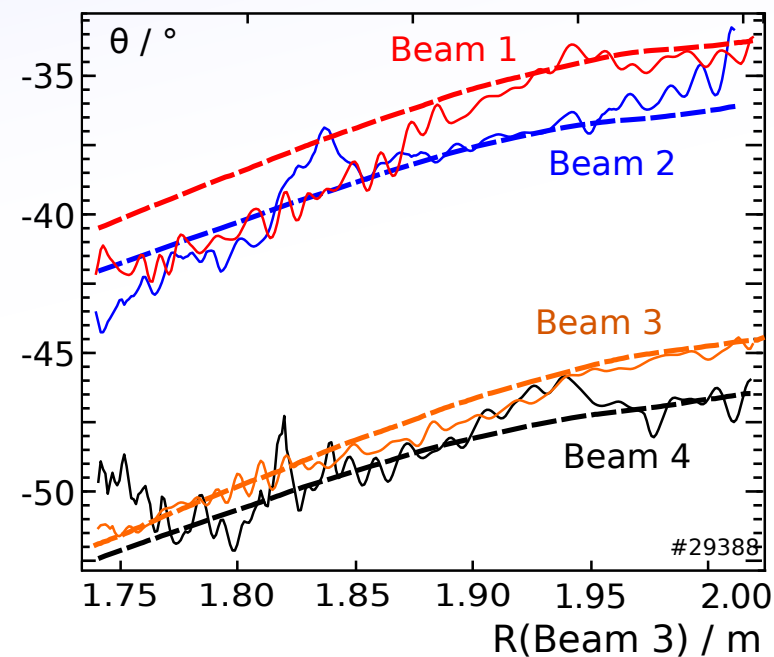
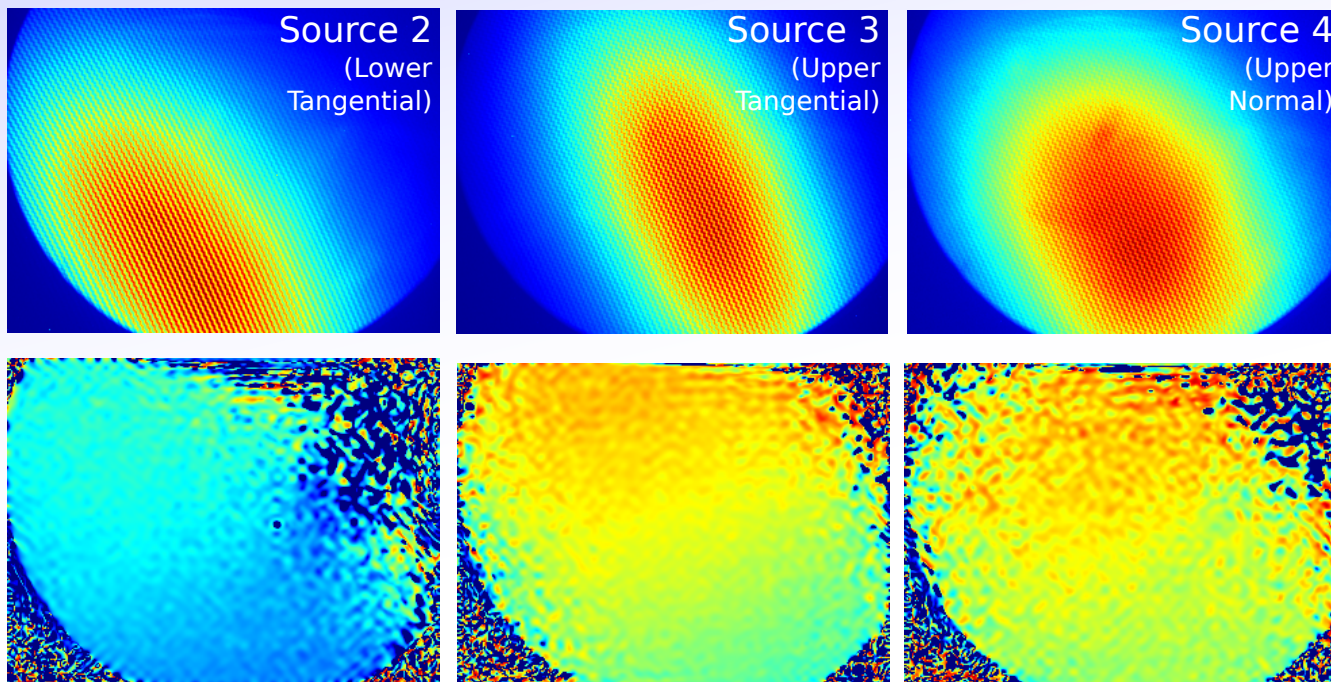
Beam Configuration Insensitivity

IMSE is insensitive to the spectrum so works on all 4 beam sources with both Deuterium and Hydrogen fuel:



Beam Configuration Insensitivity

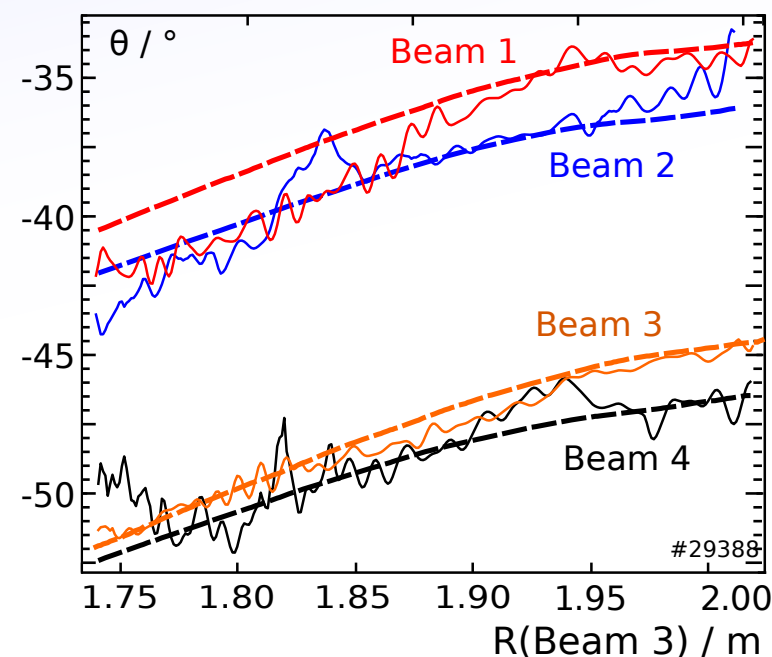
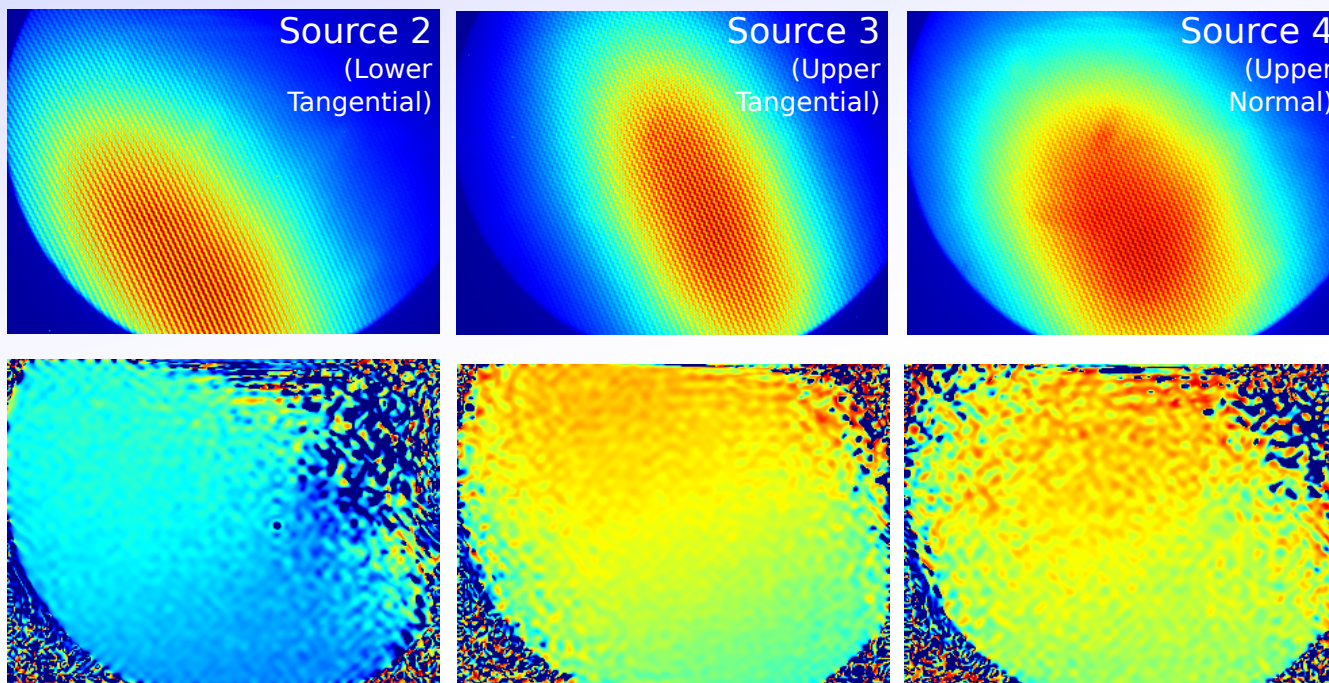
IMSE is insensitive to the spectrum so works on all 4 beam sources with both Deuterium and Hydrogen fuel:



$\theta_3 - \theta_1$ is a fixed geometry value, so the agreement confirms the diagnostic linearity and beam geometry.
 $\theta_3 - \theta_4$ (or $\theta_2 - \theta_1$) relate directly to B_z/B_ϕ and are unaffected by fixed offset errors.

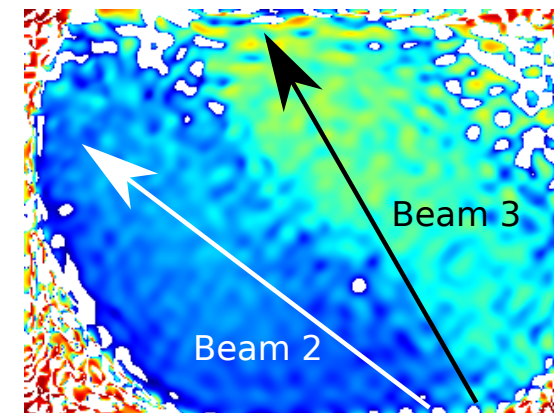
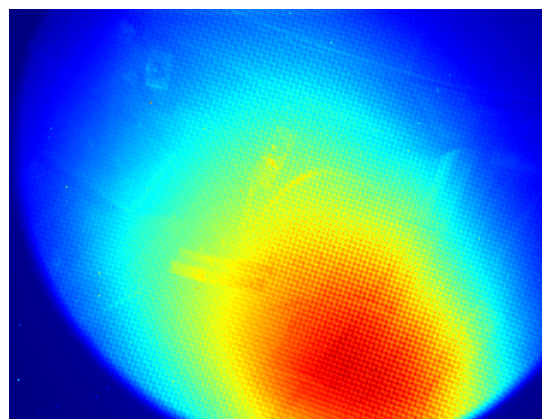
Beam Configuration Insensitivity

IMSE is insensitive to the spectrum so works on all 4 beam sources with both Deuterium and Hydrogen fuel:



$\theta_3 - \theta_1$ is a fixed geometry value, so the agreement confirms the diagnostic linearity and beam geometry.
 $\theta_3 - \theta_4$ (or $\theta_2 - \theta_1$) relate directly to B_z/B_ϕ and are unaffected by fixed offset errors.

In principle, it is also possible to use data when multiple beams are on. The data is a complex average but can be analysed with the forward model if the beam geometry model is accurate.





Summary

Conclusions:

- ✓ 2D MSE measurements increase the data quantity and also the information per data point.
- ✓ An IMSE diagnostic has been designed, constructed and operated at ASDEX Upgrade.
- ✓ Polarisation angle images were recorded over two periods with Hydrogen and Deuterium beams.
- ✓ Initial analysis shows agreement with conventional MSE for a repeated plasma.
- ✓ Forward modelling shows agreement with expected polarisation at the diagnostic, well within expected uncertainty. This implies there are no significant unexpected effects in forward optics.
- ✓ Evaluation of different beams confirm measurement linearity and provides a cross-check of pitch angle when absolute calibration is unavailable.



Summary

Conclusions:

- ✓ 2D MSE measurements increase the data quantity and also the information per data point.
- ✓ An IMSE diagnostic has been designed, constructed and operated at ASDEX Upgrade.
- ✓ Polarisation angle images were recorded over two periods with Hydrogen and Deuterium beams.
- ✓ Initial analysis shows agreement with conventional MSE for a repeated plasma.
- ✓ Forward modelling shows agreement with expected polarisation at the diagnostic, well within expected uncertainty. This implies there are no significant unexpected effects in forward optics.
- ✓ Evaluation of different beams confirm measurement linearity and provides a cross-check of pitch angle when absolute calibration is unavailable.

Next steps:

- Analysis of data with Current Tomography (\pm equilibrium assumption).
- Further improvements to signal/noise, temporal resolution.
- A calibration method is required to determine the single fixed offset with $\sim 0.1^\circ$ precision.

